Flat Potential Energy Surface of the Saturated Binuclear Homoleptic Chromium Carbonyl $Cr_2(CO)_{11}$ with One, Two, and Three Bridging Carbonyls: Comparison with the Well-Known $[HCr_2(CO)_{10}]^-$ Anion and the Related $[(\mu\text{-}H)_2Cr_2(CO)_9]^{2-}$ and $[(\mu\text{-}H)_2Cr_2(CO)_8]^{2-}$ Dianions

Nancy A. Richardson,* Yaoming Xie, R. Bruce King, and Henry F. Schaefer III

Center for Computational Quantum Chemistry, University of Georgia, Athens, Georgia 30602

Received: August 29, 2001; In Final Form: October 12, 2001

The thermodynamic stability of dichromium carbonyls is investigated with density functional theory (DFT). The results demonstrate why $[(\mu\text{-}H)Cr_2(CO)_{10}]^-$ has been observed while the $Cr_2(CO)_{11}$ and $(\mu\text{-}H)_2Cr_2(CO)_9$ structures remain unknown. The related structure $[(\mu\text{-}H)_2Cr_2(CO)_8]^{2-}$ is predicted to be stable with respect to its fragments and isolable. Homoleptic chromium carbonyl structures of the formula $Cr_2(CO)_{11}$ appear to be thermodynamically unstable with respect to dissociation to the fragments $Cr(CO)_6$ and $Cr(CO)_5$ and only slightly metastable with respect to the transition state leading to these dissociated fragments. The potential energy surface in the region adjacent to these minima appears to be very flat. In contrast, both the BP86 and B3LYP functionals predict the known $[(\mu\text{-}H)Cr_2(CO)_{10}]^-$ to have significant stability with respect to the fragments $Cr(CO)_5 + [Cr(CO)_5H]^-$. For the B3LYP functional, the dissociation energy is 41 kcal/mol, while for BP86 it is 43 kcal/mol. A notable structural difference for $[(\mu\text{-}H)Cr_2(CO)_{10}]^-$ between the two theoretical methods is that the BP86 functional predicts the Cr−H−Cr angle to be 147° while the B3LYP functional predicts a linear geometry (180°). Experimental structures of $[(\mu\text{-}H)Cr_2(CO)_{10}]^-$ determined by neutron diffraction and by X-ray crystallography display a remarkably similar ambiguity in the Cr−H−Cr angle. Certain other differences between the B3LYP and BP86 functionals are observed in the predicted geometries, numbers of imaginary vibrational frequencies, and particular energy differences. Several subtle comparisons suggest that the BP86 method is preferable to B3LYP for this particular class of compounds.

I. Introduction

While $Co_2(CO)_8$, $Fe_2(CO)_9$, and $Mn_2(CO)_{10}$ are well-known and relatively stable isolable transition metal compounds and infrared ν(CO) spectroscopic evidence indicates the existence of $V_2(CO)_{12}$ in low-temperature matrixes,[1−3] the intermediate dichromium member of this series, $Cr_2(CO)_{11}$, has never been conclusively detected. In 1975, Burdett, Graham, Perutz, Poliakoff, Rest, Turner, and Turner[4] observed a band at 1896 cm^{-1} which they postulated could belong to a $Cr_x(CO)_y$ fragment. Known related dichromium carbonyls include the following.

(1) The anion $[(\mu\text{-}H)Cr_2(CO)_{10}]^-$, which is derived from $Cr_2(CO)_{11}$ by replacement of one of the carbonyl groups with a bridging hydride (H^-) ligand, has been structurally characterized by X-ray and neutron diffraction as its Et_4N^+,[5−7] $Ph_3P{=}N{=}PPh_3^+$,[8] and K(1,10-phenanthroline)$_3^+$ salts,[9] in which the $[(\mu\text{-}H)Cr_2(CO)_{10}]^-$ anion **I** exhibits a Cr−H−Cr bond angle of

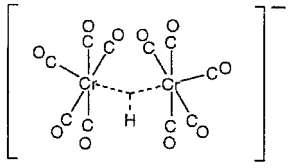

$[(\mu\text{-}H)Cr_2(CO)_{10}]^-$

I

around 159°, consistent with three-center two-electron (3c−2e) Cr−H−Cr bonding. The Cr−Cr bond length in $[(\mu\text{-}H)Cr_2(CO)_{10}]^-$ of 3.39 Å is significantly longer than the Cr−Cr bond in $[Cr_2(CO)_{10}]^{2-}$ (2.98−3.00 Å)[10−12] in accord with the origin of the 3c−2e Cr−H−Cr bond in $[(\mu\text{-}H)Cr_2(CO)_{10}]^-$. The molybdenum[13] and tungsten[14,15] analogues, $[(\mu\text{-}H)M_2(CO)_{10}]^-$ (M = Mo, W), have also been shown by X-ray diffraction to display related structures.

(2) The binuclear chromium carbonyl complex $[MeN(PF_2)_2]_3Cr_2(CO)_5$ is known.[16] This may be regarded as a substitution product of $Cr_2(CO)_{11}$ in which six of the carbonyl groups have been replaced pairwise by three small bite bidentate, strong π-acceptor $MeN(PF_2)_2$ligands.[17] A more extensive series of analogous substitution products of $Mo_2(CO)_{11}$, namely $[RN(PF_2)_2]_nMo_2(CO)_{11-2n}$ (n = 3, 4, 5) is known,[16] of which $[PhN(PF_2)_2]_3Mo_2(CO)_5$ and $[MeN(PF_2)_2]_4Mo_2(CO)_3$ have been shown by X-ray diffraction[18] to have structures **II** (R = Ph) and **III**

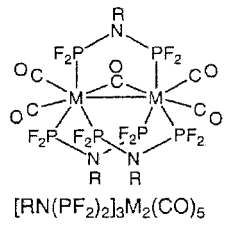

$[RN(PF_2)_2]_3M_2(CO)_5$

II

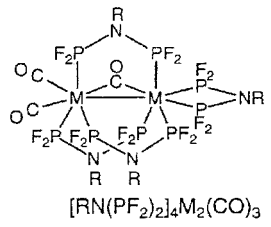

$[RN(PF_2)_2]_4M_2(CO)_3$

III

(R = Me), respectively.

The $M_2(CO)_{11}$ (M = Cr, Mo, W)-like structures appear to be stabilized in these $[RN(PF_2)_2]_nM_2(CO)_{11-2n}$ derivatives by the ability of the $RN(PF_2)_2$ ligands to form multiple five-membered M_2P_2N chelate rings containing the metal−metal

10.1021/jp013347c CCC: $20.00
Published on Web 11/15/2001

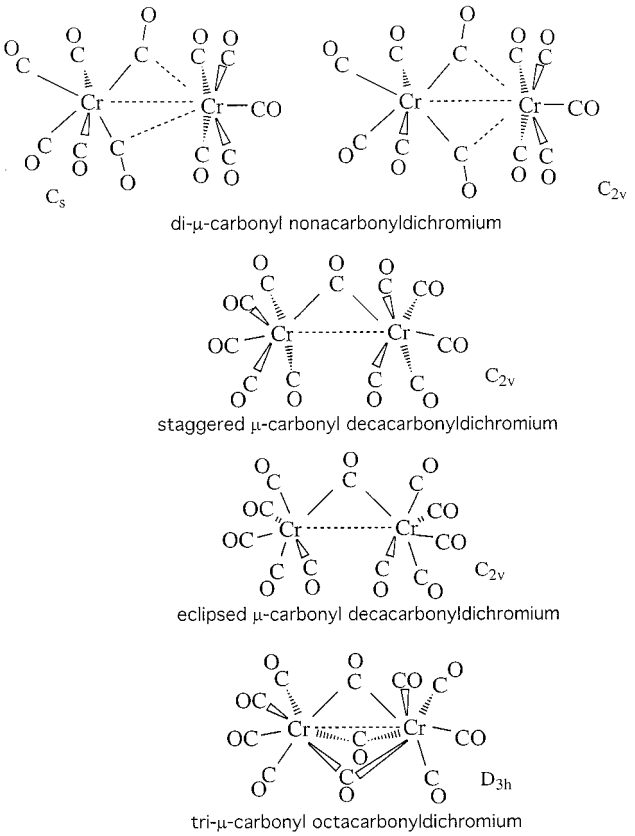

Figure 1. Five $Cr_2(CO)_{11}$ structures shown from most stable to least stable.

single bond. Requirements for small bite bidentate ligands to form such stable $M_2(CO)_{11}$ derivatives (M = Cr, Mo, W) appear to include strong π-acceptor properties,[17] since the more basic but much weaker π-acceptor ligand $CH_2(PMe_2)_2$ was found not to form analogous binuclear Group 6 metal carbonyl complexes.[19]

The lack of solid experimental evidence for the existence of $Cr_2(CO)_{11}$ may be the reason for the absence of theoretical studies of such homoleptic binuclear chromium carbonyls. This is in contrast to the homoleptic binuclear carbonyls of the other first row transition metals including nickel,[20] iron,[21] and cobalt[22], which we have recently studied by density functional methods. The related dichromium anion, $[(\mu\text{-H})Cr_2(CO)_{10}]^-$, has attracted some attention among theoretical chemists. Thus, in 1984 Eyermann and Chung-Phillips[23] reported a study of the electronic structure and the nature of the 3c−2e Cr−H−Cr bond in $[(\mu\text{-H})Cr_2(CO)_{10}]^-$ using self-consistent-field Xα scattered wave calculations. In 1988, Jezowska-Trzebiatowska and Nissen-Sobocinska[24] carried out further work using the Fenske−Hall method. These authors also studied another related structure, $[(\mu\text{-H})_2Cr_2(CO)_8]^{2-}$, using the same method,[25] though only the tungsten analogue is known experimentally.[26] The structures $Cr_2(CO)_{11}$, $[(\mu\text{-H})Cr_2(CO)_{10}]^-$, and $[(\mu\text{-H})_2Cr_2(CO)_8]^{2-}$ all appear to provide chromium with the favored 18-electron configuration[27] whether using a covalent or ionic model for counting.[28] The difference between these structures calls for exploration.

The aim of the work reported in the present paper is to use modern density functional methods to investigate the stability and possible structures of $Cr_2(CO)_{11}$ and the relationships between structures of $Cr_2(CO)_{11}$ and those of the closely related and well-known anion $[(\mu\text{-H})Cr_2(CO)_{10}]^-$. These are also compared with the related but as-yet unknown $[(\mu\text{-H})_2Cr_2(CO)_9]^{2-}$, $(\mu\text{-CO})(\mu\text{-H})_2Cr_2(CO)_8$, and $[(\mu\text{-H})_2Cr_2(CO)_8]^{2-}$ structures. We optimized the geometries of the possible structural isomers of $Cr_2(CO)_{11}$, $[Cr_2(CO)_{10}H]^-$, $[(\mu\text{-H})_2Cr_2(CO)_9]^{2-}$, $(\mu\text{-CO})(\mu\text{-H})_2Cr_2(CO)_8$, and $[(\mu\text{-H})_2Cr_2(CO)_8]^{2-}$; determined the harmonic vibrational frequencies; and compared the energies of each structure to the energies of the appropriately separated fragments. Figure 1 shows the five $Cr_2(CO)_{11}$ structures: two conformations of di-μ-carbonyl nonacarbonyldichromium, two conformations of μ-carbonyl decacarbonyldichromium, and lastly tri-μ-carbonyl octacarbonyldichromium. Figure 2 sketches the $[(\mu\text{-H})Cr_2(CO)_{10}]^-$ structures: three conformations of the μ-hydrido-decacarbonyl dichromium anion and the di-μ-carbonyl-μ-hydrido-octacarbonyl dichromium anion. Figure 3 compares the other $(\mu\text{-H})_x(\mu\text{-CO})_yCr_2(CO)_z$ structures: the dihydrido-nonacarbonyl dichromium dianion, the decacarbonyl dichromium dianion, the di-μ-hydrido-μ-carbonyl-octacarbonyl dichromium molecule, and the di-μ-hydrido-octacarbonyl dichromium dianion. In each figure, the structures are arranged from lowest energy at the top of the figure to highest energy at the bottom

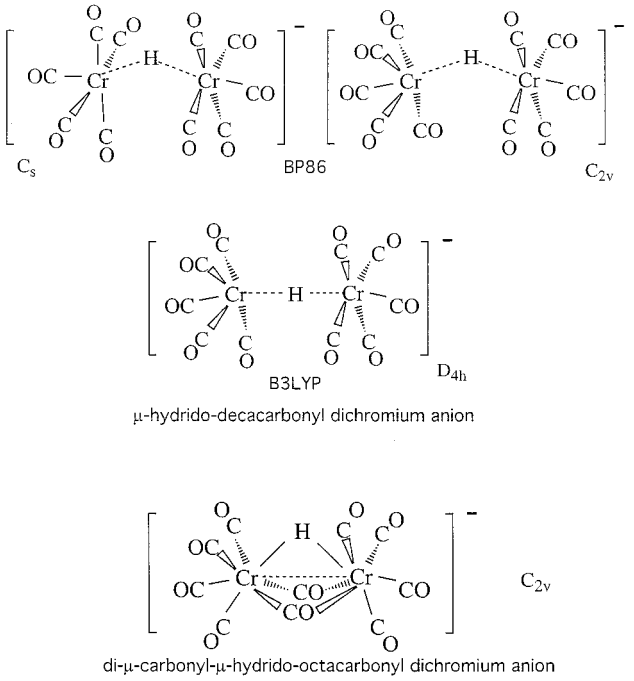

Figure 2. Five structures of $[(\mu\text{-H})Cr_2(CO)_{10}]^-$ with their symmetries.

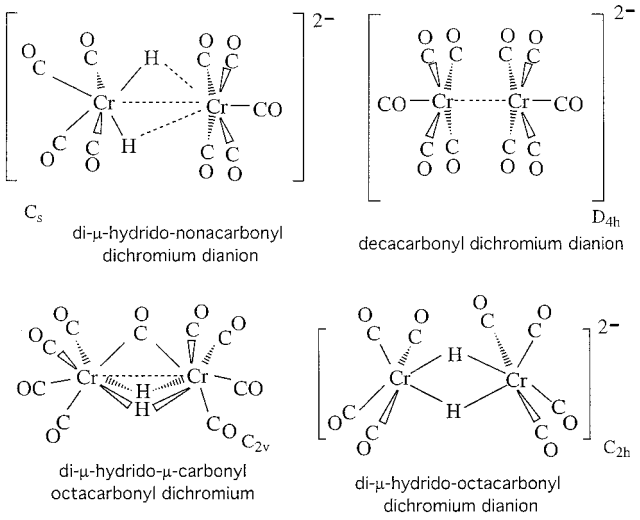

Figure 3. Four structures of $(\mu\text{-H})_x(\mu\text{-CO})_yCr_2(CO)_z$ with their symmetries.

TABLE 1: Symmetries, Number of Imaginary Vibrational Frequencies, and Total Energies for $Cr_2(CO)_{11}$ Structures

species/method	symmetry	figure	no. of imaginary frequencies	total energy (hartrees)	relative energy (kcal/mol)
$Cr(CO)_5 + Cr(CO)_6$/B3LYP	C_{4v}, O_h		0, 0[a]	−3336.023 72	0.0
staggered (μ-CO)$Cr_2(CO)_{10}$/B3LYP	C_{2v}	5	2	−3336.002 31	13.4
eclipsed (μ-CO)$Cr_2(CO)_{10}$(2)/B3LYP	C_{2v}	6	3	−3335.999 85	15.0
(μ-CO)$_3Cr_2(CO)_8$/B3LYP	D_{3h}	7	2	−3335.915 60	67.8
$Cr(CO)_5 + Cr(CO)_6$/BP86	C_{4v}, O_h		0, 0	−3336.442 45	0.0
(μ-CO)$_2Cr_2(CO)_9$/BP86	C_s	4	0	−3336.439 82	1.7
(μ-CO)$_2Cr_2(CO)_9$/BP86	C_{2v}	1	1	−3336.439 44	1.9
staggered (μ-CO)$Cr_2(CO)_{10}$/BP86	C_{2v}	5	1	−3336.433 50	5.6
eclipsed (μ-CO)$Cr_2(CO)_{10}$/BP86	C_{2v}	6	2	−3336.430 29	7.6
(μ-CO)$_3Cr_2(CO)_8$/BP86	D_{3h}	7	2	−3336.377 20	40.9

[a] For dissociation limits the symmetry and the number of imaginary vibrational frequencies for each fragment are listed in order of occurrence.

TABLE 2: Symmetries, Number of Imaginary Vibrational Frequencies, and Total Energies of (μ-H)$_x$Cr$_2$(CO)$_y$ ($x = 1, 2$; $y = 8, 10$) Structures

species/method	symmetry	figure	no. of imaginary frequencies (hartrees)	total energy (kcal/mol)	relative energy
staggered [(μ-H)$Cr_2(CO)_{10}$]$^-$/B3LYP	C_s	8	0	−3223.380 96	0.0
eclipsed [(μ-H)$Cr_2(CO)_{10}$]$^-$/B3LYP	C_{2v}	9	1	−3223.378 88	1.3
$Cr(CO)_5 + [Cr(CO)_5H]^-$/B3LYP	C_{4v}, C_{4v}		0, 0	−3223.315 88	40.8
$Cr(CO)_6 + [Cr(CO)_4H]^-$/B3LYP	O_h, C_{2v}		0, 1	−3223.290 17	57.0
[(μ-CO)$_2$(μ-H)$Cr_2(CO)_8$]$^-$/B3LYP	C_{2v}	10	1	−3223.280 47	63.0
staggered [(μ-H)$Cr_2(CO)_{10}$]$^-$/BP86	C_s	8	0	−3223.806 79	0.0
eclipsed [(μ-H)$Cr_2(CO)_{10}$]$^-$/BP86	C_{2v}	9	1	−3223.803 62	1.9
$Cr(CO)_5 + [Cr(CO)_5H]^-$/BP86	C_{4v},C_{4v}		0, 1	−3223.738 55	42.7
$Cr(CO)_6 + [Cr(CO)_4H]^-$/BP86	O_h, C_{2v}		0, 0	−3223.714 69	57.7
[(μ-CO)$_2$(μ-H)$Cr_2(CO)_8$]$^-$/BP86	C_{2v}	10	1	−3223.738 08	41.1
(μ-CO)(μ-H)$_2Cr_2(CO)_8$/B3LYP	C_{2v}	12	1	−3110.399 56	
(μ-CO)(μ-H)$_2Cr_2(CO)_8$/BP86	C_{2v}	12	1	−3110.833 16	
$[Cr(CO)_4H]^- + [Cr(CO)_5H]^-$/B3LYP	C_{2v}, C_{2v}		0, 0	−3110.583 88	0.0
$[Cr_2H_2(CO)_9]^{2-}$/B3LYP	C_{2v}	11	0	−3110.518 09	41.3
[(μ-CO)(μ-H)$_2Cr_2(CO)_8$]$^{2-}$/B3LYP	C_{2v}		1	−3110.500 55	52.3
$[Cr(CO)_4H_2]^{2-} + Cr(CO)_5$/BP86	C_{2v}, C_{4v}		0, 0	−3110.411 12	108.4
$[Cr(CO)_4H]^- + [Cr(CO)_5H]^-$/BP86	C_{4v}		0, 1	−3111.012 96	0.0
$[Cr_2H_2(CO)_9]^{2-}$/BP86	C_{2v}	11	0	−3110.958 58	34.1
[(μ-CO)(μ-H)$_2Cr_2(CO)_8$]$^{2-}$/BP86	C_{2v}		1	−3110.932 16	50.7
$[Cr(CO)_4H_2]^{2-} + Cr(CO)_5$/BP86	C_{4v}		0, 1	−3110.835 67	111.2
2 $[Cr(CO)_5]^-$/B3LYP	C_{4v}		0	3222.787 65	0.0
$[Cr_2(CO)_{10}]^{2-}$/B3LYP	C_{2v}		1	−3222.734 47	33.4
2 $[Cr(CO)_5]^-$/BP86	C_{2v}		0	−3223.220 23	0.0
$[Cr_2(CO)_{10}]^{2-}$/BP86	D_{4h}		1	−3222.173 80	29.1
[(μ-H)$_2Cr_2(CO)_8$]$^{2-}$/B3LYP	C_{2h}	13	0	−2997.177 54	0.0
2 $[Cr(CO)_4H]^-$/B3LYP	C_{2v}		0	−2997.166 70	6.8
[(μ-H)$_2Cr_2(CO)_8$]$^{2-}$/BP86	C_{2h}	13	0	−2997.177 54	0.0
2 $[Cr(CO)_4H]^-$/BP86	C_{2v}		0	−2997.590 48	7.5

of the figure. For some structures we present full figures with bond lengths and some angles. Table 1 lists the symmetry, figure number for the full figure (where one is presented), number of imaginary vibrational frequencies, total energies, and relative energies for each structure in Figure 1. Table 2 lists the same information for the structures in Figures 2 and 3. Table 3 lists the imaginary harmonic vibrational frequencies for structures which may not be minima.

TABLE 3: Imaginary Harmonic Vibrational Frequencies for Chromium Carbonyl Structures[a]

structure	mode-symmetry	B3LYP (cm^{-1})	BP86 (cm^{-1})
$[Cr(CO)_5H]^-$	b_2		16i
staggered (μ-CO)$Cr_2(CO)_{10}$	b_2	54i	
	a_2	28i	28i
eclipsed (μ-CO)$Cr_2(CO)_{10}$	b_2	94i	
	a_2	32i	34i
	b_1	31i	36i
(μ-CO)$_3Cr_2(CO)_8$	e″	176i	126i
eclipsed [(μ-H)$Cr_2(CO)_{10}$]$^-$	a_2	6i	14i
[(μ-CO)$_2$(μ-H)$Cr_2(CO)_8$]$^-$	a_2	172i	117i
[(μ-CO)(μ-H)$_2Cr_2(CO)_9$]$^{2-}$	a_2	187i	180i
(μ-CO)(μ-H)$_2Cr_2(CO)_8$	b_1	99i	109i

[a] Some of the vibrational frequencies are real for one DFT method and imaginary for the other.

II. Theoretical Methods

Our basis set for C and O begins with Dunning's standard double-ζ (DZ) contraction[29] of Huzinaga's primitive sets[30] and is designated (9s5p/4s2p). The double-ζ plus polarization (DZP) basis set used here adds one set of pure spherical harmonic *d* functions with orbital exponents $\alpha_d(C) = 0.75$ and $\alpha_d(O) = 0.85$ to the DZ basis set. For Cr, our loosely contracted DZP basis set, constructed from the Wachters' primitive Gaussian set,[31] is used, augmented by two sets of *p* functions and one set of *d* functions. This chromium basis set, contracted following Hood et al.,[32] is designated (14s11p6d/10s8p3d). For $Cr_2(CO)_{11}$, there were 428 contracted Gaussian functions in the present DZP basis set.

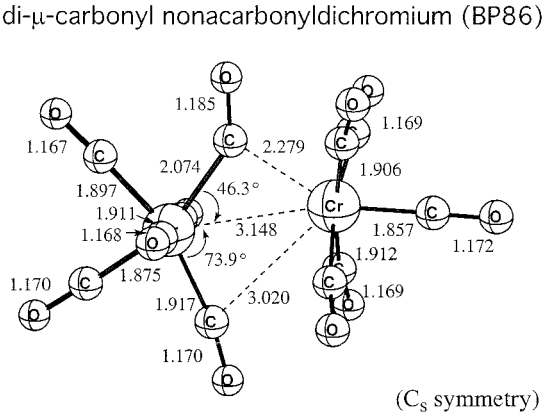

Figure 4. Minimum energy structure for $Cr_2(CO)_{11}$ with all real harmonic vibrational frequencies. Distances are reported in angstroms.

Electron correlation effects were treated employing density functional theory (DFT) methods, which have been put forth as a practical and effective computational tool, especially for organometallic compounds.[20−22,33,34] Among density functional procedures, the most reliable approximation is often thought to be the hybrid HF/DFT method using a combination of the three-parameter Becke exchange functional with the Lee−Yang−Parr nonlocal correlation functional; this is the B3LYP method.[35,36] However, another DFT method, which combines Becke's 1988 exchange functional with Perdew's 1986 nonlocal correlation functional (BP86), was also used in the present paper for comparison.[37,38]

We fully optimized the geometries of all structures using the DZP basis set with both the B3LYP and BP86 methods. At the same levels, we also computed the vibrational frequencies by evaluating analytic second derivatives of the total energy with respect to the nuclear coordinates. The computations were carried out with the Gaussian 94 program[39] in which the fine grid (75 302) was employed for numerical evaluation of integrals. In a few test cases we used a larger grid (99 590). Stationary point geometrical structures were optimized within various point group symmetry constraints using analytic gradient techniques, until residual Cartesian coordinate gradients were less than 10^{-6} a.u.

III. Results

Condensed representations of the fully optimized $Cr_2(CO)_{11}$ structures are shown in Figure 1 while complete structures of these molecules with geometric parameters are shown in Figures 4−7. At 1.7 kcal/mol higher energy than the total energy for the fragments $Cr(CO)_6$ and $Cr(CO)_5$, the structure $(\mu\text{-}CO)_2Cr_2(CO)_9$ has the lowest energy of all the $Cr_2(CO)_{11}$ structures and has all real vibrational frequencies. The lowest of the real vibrational frequencies is 14 cm^{-1}. The other $Cr_2(CO)_{11}$ structures lie close in energy and have one or more imaginary vibrational frequencies, indicating they are transition states to lower energy structures. The wave functions for all of the structures with C_{2v} symmetry correspond to the $^1A_1$ electronic states. The dibridged structure (upper left-hand corner of Figure 1) is of C_s symmetry, and the tribridged structure falls within the D_{3h} point group and is a $^1A_1'$ electronic state. Table 1 lists these structures with their symmetries, numbers of imaginary vibrational frequencies, total energies, and relative energies.

Figure 2 shows condensed representations of the fully optimized $[Cr_2(CO)_{10}H]^-$ structures, while Figure 3 shows $[Cr_2H_2(CO)_9]^{2-}$, $[Cr_2(CO)_{10}]^{2-}$, $(\mu\text{-}CO)(\mu\text{-}H)_2Cr_2(CO)_8$, and $[(\mu\text{-}H)_2Cr_2(CO)_8]^{2-}$ structures. Figures 8−10 show the $[Cr_2(CO)_{10}H]^-$ structures, Figure 11 shows $[(\mu\text{-}H)_2Cr_2(CO)_9]^{2-}$, Figure 12 shows $(\mu\text{-}CO)(\mu\text{-}H)_2Cr_2(CO)_8$, and Figure 13 shows the $[(\mu\text{-}H)_2Cr_2(CO)_8]^{2-}$ dianion. Of the two types of $[Cr_2(CO)_{10}H]^-$ structures, $[(\mu\text{-}H)Cr_2(CO)_{10}]^-$ is lower in energy and also lies

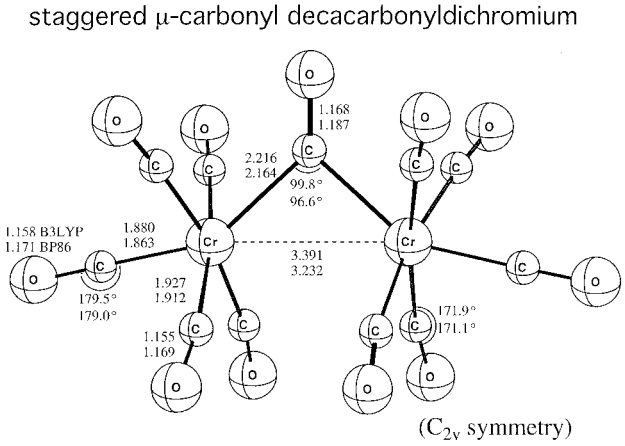

Figure 5. Second lowest energy (staggered) conformer for $Cr_2(CO)_{11}$ with one and two imaginary harmonic vibrational frequencies for BP86 and B3LYP, respectively. Distances are reported in angstroms.

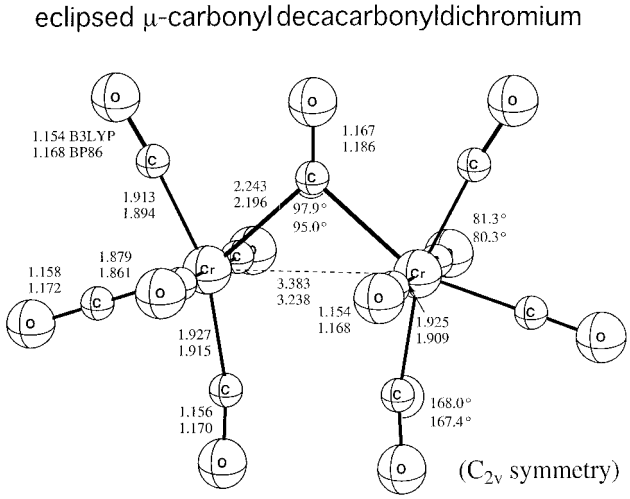

Figure 6. Third lowest energy (eclipsed) structure for $Cr_2(CO)_{11}$ with imaginary harmonic vibrational frequencies for both BP86 and B3LYP. Distances are reported in angstroms.

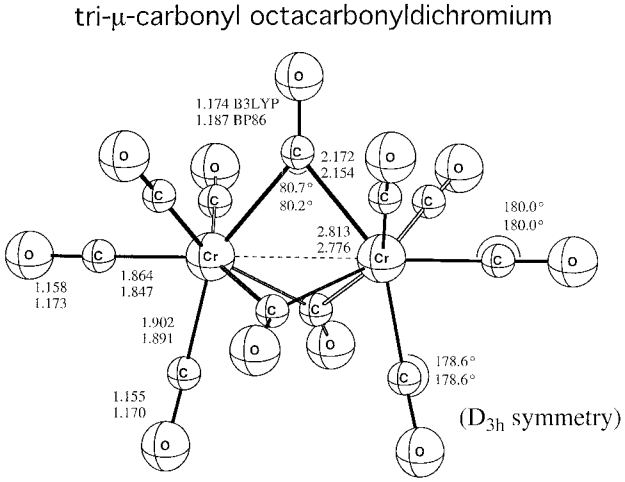

Figure 7. Tribridging conformation for $Cr_2(CO)_{11}$ with one large imaginary harmonic vibrational frequency for both BP86 and B3LYP. Distances are reported in angstroms.

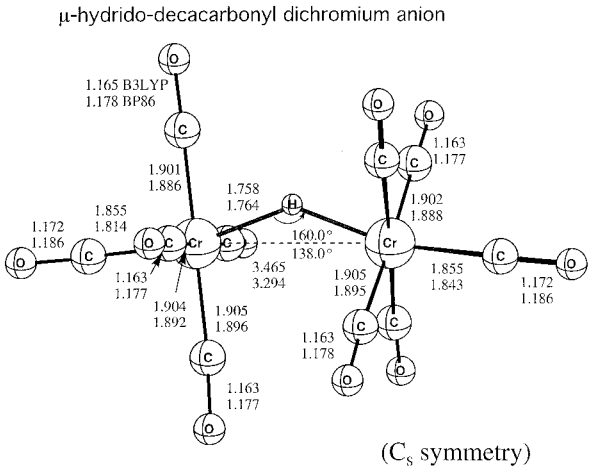

Figure 8. Staggered minimum energy structure of C_s symmetry, $[(\mu\text{-H})Cr_2(CO)_{10}]^-$. This structure has all real harmonic vibrational frequencies. Distances are reported in angstroms.

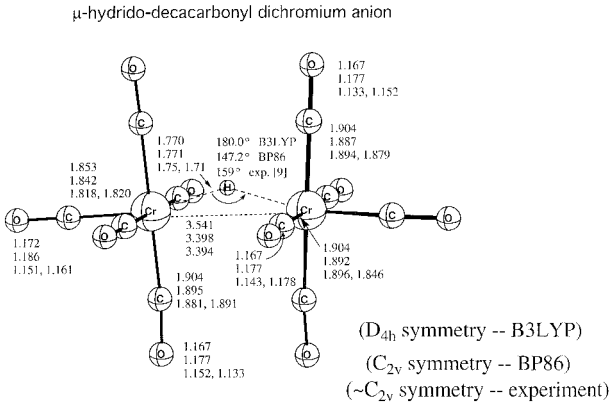

Figure 9. Eclipsed $[(\mu\text{-H})Cr_2(CO)_{10}]^-$ with one small imaginary harmonic vibrational frequency. The experimental structure which is not strictly C_{2v} is from ref 9. Distances are reported in angstroms.

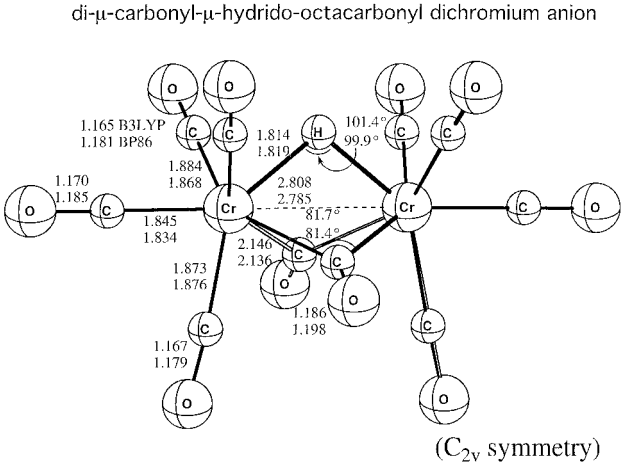

Figure 10. Tribridged $[(\mu\text{-CO})_2(\mu\text{-H})Cr_2(CO)_8]^-$ structure with one large imaginary harmonic vibrational frequency for both BP86 and B3LYP. Distances are reported in angstroms.

lower in energy than the two fragments, $Cr(CO)_6$ and $[Cr(CO)_5H]^-$, of which it is composed. The tribridging $[(\mu\text{-CO})_2(\mu\text{-H})Cr_2(CO)_8]^-$ structure lies higher in energy than its fragments. The C_s structure of $[(\mu\text{-H})Cr_2(CO)_{10}]^-$ has a $^1A'$ electronic ground state and all real vibrational frequencies. The other structures are of the C_{2v} point group and have $^1A_1$ electronic ground states; except the B3LYP structure of $[(\mu\text{-H})Cr_2(CO)_{10}]^-$ which is D_{4h} and has a $^1A_{1g}$ electronic ground

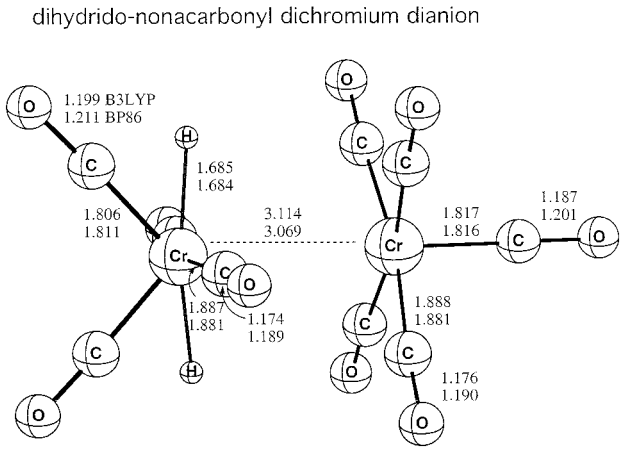

Figure 11. $[Cr_2H_2(CO)_9]^{2-}$ structure with all real harmonic vibrational frequencies for both BP86 and B3LYP. Distances are reported in angstroms.

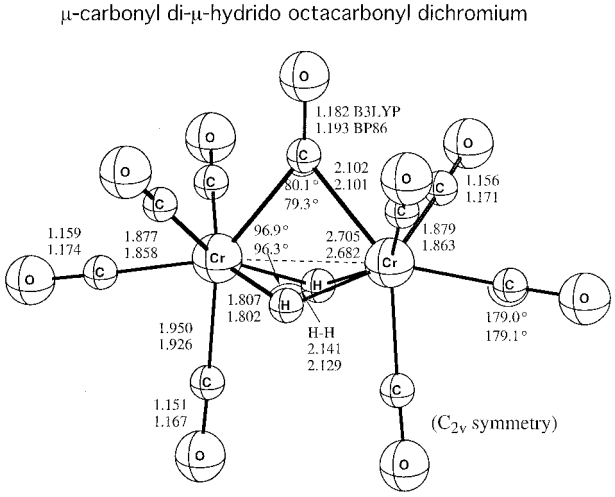

Figure 12. Tribridged $(\mu\text{-CO})(\mu\text{-H})_2Cr_2(CO)_8$ with one large imaginary harmonic vibrational frequency for BP86 and B3LYP. Distances are reported in angstroms.

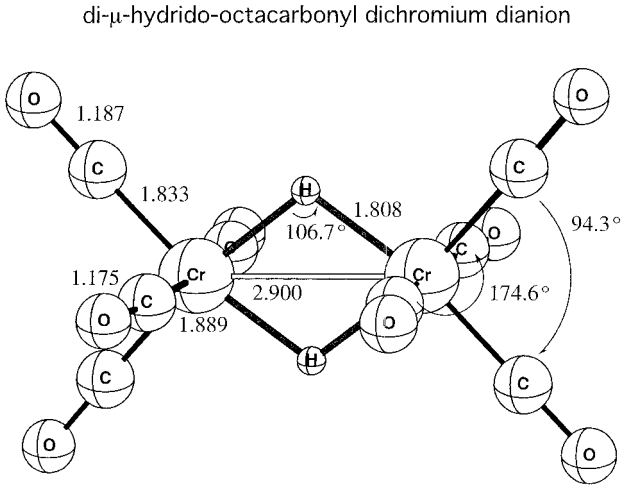

Figure 13. Dibridged $[(\mu\text{-H})_2Cr_2(CO)_8]^{2-}$ with all real harmonic vibrational frequencies for both BP86 and B3LYP. Distances are reported in angstroms.

state. These latter two C_{2v} and D_{4h} structures for $[(\mu\text{-H})Cr_2(CO)_{10}]^-$ have one or more imaginary vibrational frequencies. Table 2 lists the structures with their symmetries, numbers of imaginary vibrational frequencies, total energies, and relative energies.

TABLE 4: Comparison of Theoretical Results and Experiment for the Geometrical Parameters of $Cr(CO)_6$

	r(Cr−C) (Å)	r(C−O) (Å)
B3LYP/DZP[a]	1.923	1.155
BP86/DZP[a]	1.907	1.169
B3P86/6-311G+(d)[b]	1.901	1.141
BP86/6-311G+(d)[b]	1.911	1.156
B3LYP/6-311G+(d)[b]	1.927	1.142
BP86/ECP2[c]	1.911	1.156
HCTH/TZ2P[d]	1.907	1.148
MP2/6-31G(d)[e]	1.883	1.168
CASMP2/DZP++[f]	1.906	1.160
MCPF(T)/TZP[g]	1.940	1.178
CCSD/DZP[h]	1.950	1.168
CCSD(T)/DZP[h]	1.939	1.178
exp[i]	1.916 ± 0.002	1.140 ± 0.003
exp[j]	1.914 ± 0.002	1.140 ± 0.002

[a] This work. [b] Ref 44. [c] Ref 45. [d] Ref 41. [e] Ref 46. [f] Ref 40. [g] Ref 48. [h] Refs 48 and 47. [i] Ref 42. [j] Ref 43.

The entire potential energy surface for these molecules appears to be very flat. The values of the imaginary harmonic vibrational frequencies are listed in Table 3. Optimizations and vibrational frequency analyses were also computed with a larger grid (99 590). This produced identical geometries and harmonic vibrational frequencies compared to the results with the default (75 302) grid. However, in some of these cases, the very low vibrational frequencies may still be the result of numerical instabilities and not indicative of the precise character of a particular stationary point on the potential energy surface.

A. Fragment Analysis: $Cr(CO)_6$, $Cr(CO)_5$, $[Cr(CO)_5H]^-$, and $[Cr(CO)_4H]^-$: A Test of the Theory. To attempt to confirm the validity of the DFT functionals B3LYP and BP86 with the chosen basis set for the dinuclear chromium carbonyl structure studied here, our results are compared with results from previous work on $Cr(CO)_6$. This molecule is considered to be a demanding test of theory.[40,41] Geometries of $Cr(CO)_6$ were determined with the B3LYP and BP86 methods and were found to be in good agreement with previous experimental[42,43] and theoretical studies. These include work that employed various DFT functionals and basis sets[41,44,45]; MP2[46]; and two studies comparing MCPF, CASMP2, CCSD, and CCSD(T).[47,48] The best DFT study is Menconi, Wilson, and Tozer's recent work[41] on $Cr(CO)_6$ that employed the HTCH functional and used a TZ2P basis for the C and O (larger than the DZP in this work) and Wachter's basis set[31] for the chromium (essentially the same used in this work); the results are similar to ours. Barnes, Liu, and Lindh[48] used coupled cluster singles and doubles including a perturbational estimate for connected triple excitations [CCSD(T)] with a DZP quality basis set (which may, in fact, be too small for this highly correlated method.) Table 4 shows the variations among these results. Compared to experiment our results for the bond lengths of Cr−C and C−O differed by about 0.006 and 0.014 Å, respectively, for the B3LYP method and by about 0.010 and 0.028 Å for the BP86 method. Similar variations occurred with the HCTH method; in fact the Cr−C bond distance is identical for the BP86 functional and the HCTH functional. CCSD(T)/DZP tends to lengthen the bonds compared to experiment; we suspect that with a larger basis set, the CCSD(T) structure would be essentially indistinguishable from experiment.

While no experimental bond lengths are available for $Cr(CO)_5$, our BP86 results are similar to those of Barnes et al.[48] obtained with CCSD(T). This comparison is shown in Table 5. Our DFT bond lengths are an average of about 0.02 Å shorter than the CCSD(T) results, similar to the differences found for $Cr(CO)_6$. $Cr(CO)_5$ has a C_{4v} symmetry minimum energy structure with all real harmonic vibrational frequencies.

Since our results for $Cr(CO)_6$ and $Cr(CO)_5$ agree well with previous studies, we conclude our use of B3LYP and BP86 methods to be a reasonable choice to study $Cr_2(CO)_{11}$. The sum of the total energies for separated $Cr(CO)_6$ and $Cr(CO)_5$ molecules is the lowest energy for the $Cr_2(CO)_{11}$ potential energy surface.

Also, to obtain the dissociation energies of the $[Cr_2(CO)_{10}H]^-$ and $[(\mu\text{-}H)_2Cr_2(CO)_8]^{2-}$ structures, the total energies of the fully optimized $[Cr(CO)_4H]^-$ and $[Cr(CO)_5H]^-$ anion fragments were obtained. The $[Cr(CO)_4H]^-$ anion optimizes to a C_{2v} structure with all real harmonic vibrational frequencies for both functionals. To our knowledge, no experimental or theoretical work has previously been done on $[Cr(CO)_4H]^-$. In contrast, the experimental structure of $[Cr(CO)_5H]^-$ is known to be C_{4v}.[49] Optimization with the B3LYP functional produces a structure in good agreement with experiment and all real harmonic vibrational frequencies. Optimization with the BP86 functional gives a structure in even closer agreement with experiment, but with one very small imaginary harmonic vibrational frequency of 16i cm^{-1}. Comparison of the geometrical parameters for these structures is shown in Table 6. The Cr−C and Cr−H bond distances agree to within 0.01 Å, while the C−O bond distances agree with experiment to within 0.04 Å. The differences between the experimental and BP86 distances are identical for the axial and equatorial Cr−C. The angles also agree closely. This and several other subtle comparisons in previous work[21,22,33,45,50] suggest that the BP86 method is slightly preferable to B3LYP for this particular class of compounds; however, both of these functionals produce better results than other combinations of exchange and correlation functionals such as B3P86 or BLYP. One explanation for the slightly poorer performance of the hybrid B3 exchange functional is that it is fit to a set of mostly organic molecules. If a set of inorganic and organometallic compounds was fit, then this functional might perform better for these compounds.

Since the B3LYP functional does not predict an imaginary vibrational frequency for $[Cr(CO)_5H]^-$, the BP86 imaginary harmonic vibrational frequency probably does not correctly represent a true saddle point on the potential energy surface. This may be rather a theoretical or numerical weakness in the latter DFT method. In support of this, we found that lowering the symmetry to C_{2v} produces a structure with identical energy and the imaginary vibrational frequency persists. We conclude that using the C_{4v} structure to determine the thermodynamics is reasonable for the dissociation of the $[Cr_2(CO)_{10}H]^-$ structures.

TABLE 5: Comparison of Theoretical Results with for the Geometrical Parameters of $Cr(CO)_5$

	$r(Cr-C)_{ax}$ (Å)	$r(C-O)_{ax}$ (Å)	$r(Cr-C)_{eq}$ (Å)	$r(C-O)_{eq}$ (Å)	$\angle C_{ax}CrC_{eq}$ (deg)	$\angle CrC_{eq}O_{eq}$ (deg)
B3LYP/DZP	1.854	1.162	1.923	1.156	90.9	178.4
BP86/DZP[a]	1.829	1.177	1.905	1.171	90.1	177.6
CCSD(T)/DZP[b]	1.880	1.174	1.941	1.174	92.5	179.4

[a] This work. [b] Ref 48.

TABLE 6: Comparison of Theoretical Results and Experiment for the Geometrical Parameters of $[Cr(CO)_5H]^-$

	$r(Cr-C)_{ax}$ (Å)	$r(C-O)_{ax}$ (Å)	$r(Cr-C)_{eq}$ (Å)	$r(C-O)_{eq}$ (Å)	r(Cr−H) (Å)	$\angle C_{ax}CrC_{eq}$ (deg)	$\angle x\ CrC_{eq}O$ (deg)
B3LYP/DZP[a]	1.866	1.177	1.885	1.171	1.659	96.7	177.1
BP86/DZP[a]	1.863	1.190	1.876	1.185	1.654	96.9	177.2
exp[b]	1.852	1.152	1.865	1.145	1.66(5)	95.4	178.1

[a] This work. [b] Ref 49.

B. $Cr_2(CO)_{11}$ Structures. *1. Minimum Energy Dibridged Structure: $(\mu\text{-}CO)_2Cr_2(CO)_9$.* With the BP86 functional, the minimum energy structure of the fully optimized $Cr_2(CO)_{11}$ molecule is $(\mu\text{-}CO)_2Cr_2(CO)_9$ (C_s symmetry) and is shown in Figure 4. Using the B3LYP functional, the fragments dissociate without any barrier; since B3 includes a component of HF, the effect of the lack of electron correlation is seen in the lack of a minimum. However, with the BP86 functional, this structure is a minimum and has all real vibrational frequencies. It is composed of a $Cr(CO)_5$ fragment and a $Cr(CO)_6$ fragment with a distance of 3.148 Å between the chromium atoms. Two carbonyls from the $Cr(CO)_6$ fragment are asymmetrically bridging and lie in staggered positions with respect to the carbonyls of the $Cr(CO)_5$ fragment. The $Cr(CO)_5$ fragment retains the same symmetry and nearly the same structural parameters as the isolated $Cr(CO)_5$ molecule. In the complex the axial Cr−C bond lengthens by (1.857−1.829) = 0.028 Å from the isolated fragment while the equatorial bond remains the same. The $Cr(CO)_6$ fragment distorts so that the two asymmetrically bridging carbonyls bend toward the $Cr(CO)_5$, one carbonyl bending more than the other. The Cr−C distance of the more pronouncedly bridging carbonyl and its C−O bond both lengthen with respect to the isolated $Cr(CO)_6$ molecule. The Cr−C distance is (2.074−1.907) = 0.167 Å longer, while the C−O is only (1.185−1.169) = 0.016 Å longer. The other Cr−C bonds are slightly shorter than in the isolated $Cr(CO)_6$.

A C_{2v} dibridged structure (upper right of Figure 1) lies only 0.2 kcal/mol higher in energy than the C_s $(\mu\text{-}CO)_2Cr_2(CO)_9$ structure and has a low imaginary vibrational frequency of 13i cm^{-1}. Shown in Figure 1 is this transition structure of C_{2v} symmetry in which the bridging carbonyls are equivalent. This structure connects two C_s $(\mu\text{-}CO)_2Cr_2(CO)_9$ structures where the bridging carbonyls are inequivalent. The energy difference between this structure and the true minimum is so small that other structures with imaginary vibrational frequencies may be assumed to be reasonably close to a real minimum. Indeed the numerical uncertainties associated with DFT may make determination of the genuine minimum uncertain.

Although the BP86 functional predicts $(\mu\text{-}CO)_2Cr_2(CO)_9$ to be a local minimum, it lies 1.7 kcal/mol higher than the separated $Cr(CO)_5$ and $Cr(CO)_6$. Thus, this species is not stable thermodynamically. However, it may be stable kinetically if there is a substantial energy barrier for its dissociation. Figure 14 shows an energy curve for $(\mu\text{-}CO)_2Cr_2(CO)_9$ with respect to the Cr−Cr distance. At each fixed Cr−Cr distance, the other geometric parameters were optimized. We found that another electronic state exists, the energy of which descends more steeply as the Cr−Cr distance increases. The two states have different HOMOs. The a′ HOMO orbital of state 1, the short Cr−Cr distance, is composed of different orbitals from that of state 2, the long Cr−Cr distance. Since the Kohn−Sham theory treats the electron density with a single set of occupied orbitals, these two states fail to mix, and the two curves cross. Nevertheless, the real transition state (or a rather flat point on the surface, if the saddle point disappears with a more complete theoretical treatment) should be close to this crossing point. The crossing point has a Cr−Cr distance of 3.83 Å and an energy

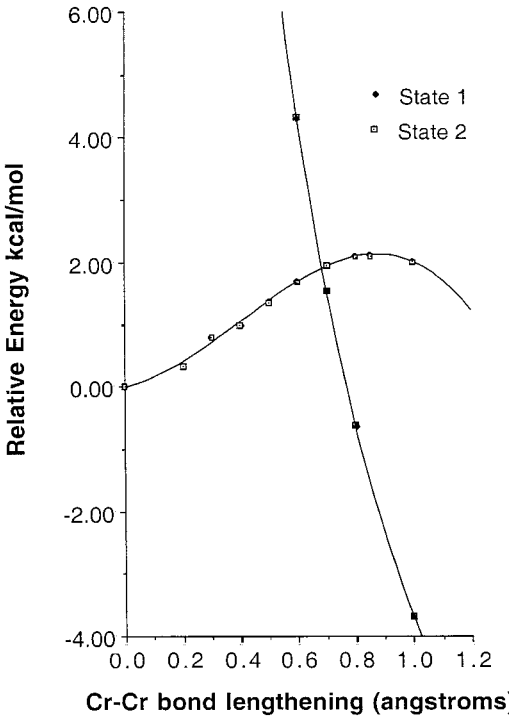

Figure 14. Energy change with Cr−Cr bond stretching. The HOMO and LUMO, both of a′ symmetry, cross as $(\mu\text{-}CO)Cr_2(CO)_{10}$ is separated into $Cr(CO)_5$ and $Cr(CO)_6$ fragments.

1.9 kcal/mol higher than the minimum energy equilibrium C_s structure of $(\mu\text{-}CO)_2Cr_2(CO)_9$. This may be regarded as the energy barrier predicted by the BP86 method. Actually, this barrier is so low that, if the $(\mu\text{-}CO)_2Cr_2(CO)_9$ molecule could be made, it would exist only at very low temperatures.

One other aspect of the $(\mu\text{-}CO)_2Cr_2(CO)_9$ structure is worthy of mention and may explain the instability of this complex. We assume that each chromium atom has 18 electrons and only the closer of the two carbonyls in bridging positions interacts with the $Cr(CO)_5$ fragment. The electrons can be counted as follows. In the $Cr(CO)_6$ fragment, the chromium acquires the favored 18-electron configuration by six electrons from itself, two from each of the five nonbridging carbonyls (10 electrons), one from the chromium of the $Cr(CO)_5$ fragment, and one from the bridging carbonyl. The chromium in the $Cr(CO)_5$ fragment acquires 18 electrons similarly. Even though two carbonyls bend toward the $Cr(CO)_5$ fragment, only one can formally interact and still preserve the favored 18-electron configuration. Any possible bonding scheme would require at least one chromium atom in $(\mu\text{-}CO)_2Cr_2(CO)_9$ to be formally seven-coordinate, which may be responsible in part for the thermodynamic instability of the structure. However, this unsymmetrical dibridging structure may be able to alleviate this somewhat by two partial 3c−2e bonds in which both bridging carbonyls interact with both chromiums but to different extents, and so the dibridging structure is favored over the strictly monobridging structures, which are considered next.

2. Monobridged $(\mu\text{-}CO)Cr_2(CO)_{10}$ Structures. In the absence of experimental or theoretical information, this would have been

the expected structure of $Cr_2(CO)_{11}$. Two monobridged (μ-CO)-$Cr_2(CO)_{10}$ structures of C_{2v} symmetry are shown in Figures 5 and 6. The difference between the two structures is that the bridging carbonyl is staggered between two of the carbonyls on each side of the molecule in the Figure 5 structure, while the bridging carbonyl in the Figure 6 structure lies in the same plane and is eclipsed with a carbonyl on each side of the molecule. The B3LYP functional predicts the staggered molecule to lie 13.4 kcal/mol higher in energy than the separated $Cr(CO)_6$ and $Cr(CO)_5$ fragments. For the BP86 functional, it lies 5.6 kcal/mol higher in energy. The eclipsed molecule in Figure 6 lies 15.0 and 7.6 kcal/mol higher in energy than the separated species for the B3LYP and the BP86 functionals, respectively. Thus, the staggered structure is favored energetically over the eclipsed by about 2 kcal/mol with both DFT methods.

The structures also differ in the number of imaginary vibrational frequencies predicted by the two functionals. This corresponds to a lowering of the symmetry toward the true minimum, the C_s (μ-CO)$_2$Cr$_2$(CO)$_9$ structure. The staggered structure has one imaginary vibrational frequency for the BP86 functional and two imaginary vibrational frequencies for the B3LYP functional. The eclipsed structure has two imaginary vibrational frequencies for the BP86 functional and three imaginary vibrational frequencies for the B3LYP functional. Several real vibrational frequencies are also very small, showing that the whole molecule is very floppy and has a rather flat potential surface with very low barriers to changes in conformation.

The reason for the lower stability of these monobridged structures may be that $Cr_2(CO)_{11}$ is more stable as a complex of weakly interacting $Cr(CO)_6$ and $Cr(CO)_5$ where one of the chromiums has the stable six-coordinate $Cr(CO)_6$ form and only one is of the less stable $Cr(CO)_5$ form, rather than as two Cr-$(CO)_5$ fragments in competition for a bridging carbonyl. The $Cr(CO)_6$ and $Cr(CO)_5$ complex may be more effective in sharing electron density through delocalized bonding involving the two bridging carbonyls thereby minimizing the seven-coordinate crowding that becomes necessary with the monobridged structures.

3. Tribridged (μ-CO)$_3$Cr$_2$(CO)$_8$ Structure. One other structure of significantly higher energy for $Cr_2(CO)_{11}$ was also found, namely the tribridged D_{3h} (μ-CO)$_3$Cr$_2$(CO)$_8$. The different results of the hybrid versus the pure exchange functional, B3LYP versus BP86 functionals, are noticeable in the different relative energies for this structure, which is shown in Figure 7. For B3LYP, this tribridged structure lies 68 kcal/mol higher than the separated $Cr(CO)_5$ and $Cr(CO)_6$ fragments, while it is only 41 kcal/mol higher for BP86. For each functional, this structure has a substantial doubly degenerate e″ imaginary harmonic vibrational frequency, 176i for B3LYP and 126i for BP86. This mode corresponds to a distortion in which two of the three bridging carbonyls move closer to one side of the molecule and the third carbonyl moves closer to the other side. The fragments dissociate along this mode.

C. Experimentally Known $[Cr_2(CO)_{10}H]^-$: A Comparison with Theory. *1. [(μ-H)Cr$_2$(CO)$_{10}$]$^-$Structure: The Known and Stable Anion.* The most notable feature of this structure is its thermodynamic stability with respect to its fragments. With the B3LYP functional, $[(\mu\text{-H})Cr_2(CO)_{10}]^-$ lies 41 kcal/mol lower in energy than the total energy for $Cr(CO)_5 + [Cr(CO)_5H]^-$ and 57 kcal/mol lower in energy than $Cr(CO)_6 + [Cr(CO)_4H]^-$. The BP86 functional gives similar results: $[(\mu\text{-H})Cr_2(CO)_{10}]^-$ is 43 kcal/mol lower than $Cr(CO)_5 + [Cr(CO)_5H]^-$ and 58 kcal/mol lower than $Cr(CO)_6 + [Cr(CO)_4H]^-$. These energetics explain why the $[(\mu\text{-H})Cr_2(CO)_{10}]^-$ anion has been isolated experimentally as a stable species.

The lowest energy conformation of $[(\mu\text{-H})Cr_2(CO)_{10}]^-$ is of C_s symmetry and is shown in Figure 8. The carbonyls on the two fragments are staggered with respect to each other. This structure has no imaginary vibrational frequencies for either functional. The Cr−H−Cr bond angle is 160° and the Cr−Cr bond distance is 3.47 Å for the B3LYP functional. The parameters are 138° and 3.29 Å for the BP86 functional. This conformation, however, is not observed in the crystal structure of the anion, where the eclipsed structure is found, perhaps owing to crystal packing forces.

Figure 9 shows the structure of the eclipsed conformation of $[(\mu\text{-H})Cr_2(CO)_{10}]^-$ that is observed in the solid phase. The two DFT functionals optimize to different symmetries. The BP86 functional predicts the Cr−H−Cr angle to be 147°, in closer agreement with the neutron diffraction experiments of Dahl et al.[6] (159°) and Petersen et al.[8] (158°), and also the X-ray diffraction experiment of Bombieri et al.[9] (159°). Ground-state self-consistent field Xα scattered wave calculations also suggested that the Cr−H−Cr bond was likely bent.[23] The B3LYP functional predicts 180°, which agrees with the earlier X-ray diffraction experiments of Handy and co-workers.[5,7] The actual experimental angle depends on the particular cation (counterion) in the ionic structure under examination. The theoretical structure depends on which functional is used. Both experiment and theory thus suggest that the Cr−H−Cr bending potential is very flat.

The Cr−Cr distance of 3.398 Å determined by BP86 agrees very well with all the experimental values: 3.386, 3.390, and 3.394 Å, respectively.[6,8,9] The structure with the linear Cr−H−Cr predicted by the B3LYP method shows more variation in Cr−Cr distance. The theoretical value is 3.541 Å while the experimental Cr−Cr distance is 3.41 Å for both experiments.[5,7] The Cr−C bond lengths agree well with experiment for both functionals, although the BP86 distances are even closer to the laboratory distances than the B3LYP. The C−O distances are on average 0.03 Å longer than experiment for both functionals. The experiments, of course, refer to the solid phase and the theoretical results to the isolated molecular anion. This could also explain the difference in the Cr−H−Cr angle between BP86 and the experiment. The BP86 functional gives a Cr−H−Cr angle of 147° while the experimental value is 159°. Overall, the experimental and theoretical results agree satisfactorily.

The experimental structure is nearly C_{2v}, but not quite. This asymmetry, if it is real, might explain why both functionals produce one very small a_2 imaginary harmonic vibrational frequency: 6i for B3LYP and 14i for BP86. This mode corresponds to a twisting of the $Cr(CO)_5$ fragments. Another possibility is that this imaginary vibrational frequency arises from numerical imprecision. If a slightly distorted structure corresponds to the real minimum, it lies too close in energy to be determined with certainty.

2. [(μ-CO)$_2$(μ-H)Cr$_2$(CO)$_8$]$^-$ Structure: An Unstable Molecule with Respect to its Fragments. The structure with two bridging carbonyls and one bridging hydrogen, [(μ-CO)$_2$(μ-H)-$Cr_2(CO)_8]^-$ shown in Figure 10, lies much higher than the above-discussed $[(\mu\text{-H})Cr_2(CO)_{10}]^-$ (63 kcal/mol for B3LYP and 41 kcal/mol for BP86) and just slightly higher than the dissociated fragments, $Cr(CO)_5 + [Cr(CO)_5H]^-$, 24 kcal/mol for B3LYP and only 2 kcal/mol for BP86. The reason for the difference between the functionals lies in the different treatments of exchange.

Both functionals produce one relatively large a_2 imaginary vibrational frequency for this tribridged structure. For B3LYP, this frequency is 172i cm^{-1}, and for BP86, it is 117i cm^{-1}. This frequency is similar to that predicted for $(\mu\text{-CO})_3Cr_2(CO)_8$ in that it corresponds to a movement of one of the bridging carbonyls toward one side of the molecule and the second toward the other side; the H is essentially stationary.

D. Stability Effects: Further Carbonyl Replacement and Change of Bond Type. *1. Carbonyl Replacement.* Effects of replacing carbonyls with two electrons or hydrides were briefly explored by determining the structures of $[Cr_2(CO)_{10}]^{2-}$ where the bridging carbonyl is replaced with two electrons, dibridging $[Cr_2H_2(CO)_9]^{2-}$ where two carbonyls are replaced with two hydrides, and tribridging $[(\mu\text{-CO})(\mu\text{-H})_2Cr_2(CO)_9]^{2-}$ where there are three bridging groups instead of two for the same carbonyl replacement. Figure 3 shows condensed representations for all of these structures while Figure 11 shows a detailed representation of dibridging $[Cr_2H_2(CO)_9]^{2-}$. Table 2 lists the relative energies of these structures with respect of their fragments. The energy of two $Cr(CO)_5^-$ fragments is about 33 kcal/mol lower than $[Cr_2(CO)_{10}]^{2-}$. The $D_{4h}[Cr_2(CO)_{10}]^{2-}$ (known experimentally)[7] does have one very small imaginary vibrational frequency of 16i cm^{-1} which is small enough to be attributed to numerical difficulties of DFT and not necessarily corresponding to symmetry lowering. The two $[(\mu\text{-H})_2Cr_2(CO)_9]^{2-}$ structures are also higher lying than the fragments $[Cr(CO)_4H]^- + [Cr(CO)_5H]^-$. The nonbridging structure is 41 kcal/mol higher for the B3LYP functional and 34 kcal/mol higher for the BP86 functional, and has all real vibrational frequencies. The tribridging structure lies much higher at 108 and 111 kcal/mol for B3LYP and BP86, respectively; it also has a large imaginary vibrational frequency similar to the other tribridging structures. Replacing the carbonyls increases the stability to a certain extent; however, the structures remain thermodynamically unstable with respect to their fragments.

2. Change of Bond Type. When the two electrons are removed from $[Cr_2H_2(CO)_9]^{2-}$, the result is the neutral structure $(\mu\text{-CO})(\mu\text{-H})_2Cr_2(CO)_8$ shown in Figure 12. Like the other two tribridging structures, it is predicted to have a notable b_1 imaginary vibrational frequency using either functional, namely 99i cm^{-1} for B3LYP and 109i cm^{-1} for BP86. However, unlike the vibrations for the other tribridging species, this vibration is a twisting of the nonbridging carbonyls around the Cr−Cr axis. This large imaginary harmonic vibrational frequency leads us to predict that $(\mu\text{-CO})(\mu\text{-H})_2Cr_2(CO)_8$ is less stable than its fragments $Cr(CO)_5 + Cr(CO)_4$.

The computed structure for $(\mu\text{-CO})(\mu\text{-H})_2Cr_2(CO)_8$ is closely related to the experimentally determined structures of the well-known diborane,[51] B_2H_6 or $(\mu\text{-H})_2B_2H_4$, and the known,[52,53] stable trinuclear osmium carbonyl $(\mu\text{-H})_2Os_3(CO)_{10}$ (Figure 13). All three structures have the same type of central $M_2(\mu\text{-H})_2$ unit, which can be formulated with two three-center two-electron (3c−2e) M−H−M bonds. For electron-counting purposes, these 3c−2e M−H bonds may be dissected into a dative bond composed of two electrons in a 2c−2e M−H bond to the second metal atom by overlap of the 2c−2e M−H bonding orbital with a hybrid orbital from the second metal atom to form the 3c−2e bond (Figure 15). This dissection of the 3c−2e M−H−M bond is analogous to the formulation of the metal−ligand bond in a metal−dihydrogen complex[27,54] as a dative bond from the electron pair of the H−H σ-bond in H_2 to an empty metal atom orbital. Using this formalism, the chromium atoms in $(\mu\text{-CO})(\mu\text{-H})_2Cr_2(CO)_8$ acquire the favored 18-electron noble gas configuration by having six of its own electrons, receiving eight

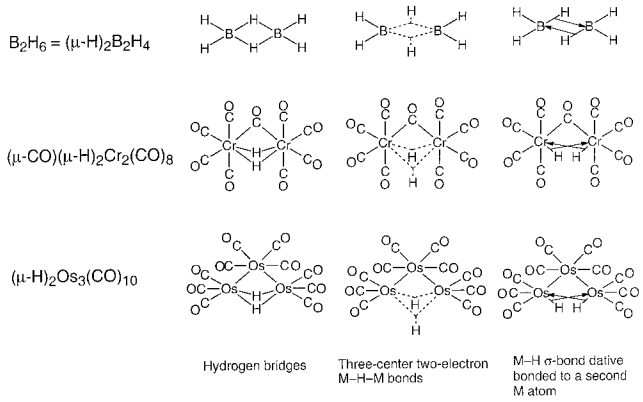

Figure 15. A comparison of B_2H_6, $(\mu\text{-CO})_2Cr_2(CO)_9$, and $(\mu\text{-H})_2Os_3(CO)_{10}$ depicting the central $M_2(\mu\text{-H})_2$ units as simple hydrogen bridges, as two 3c−2e M−H−M bonds, and as M−H σ-bonds dative bonding to the second M atom.

electrons from the four terminal CO groups, one electron from the shared bridging CO group, one electron from the hydrogen atom assumed to be bonded to the Cr initially by a 2c−2e M−H bond, and two electrons from a dative bond from the M−H bond involving the second metal atom (see Figure 13). The Cr−Cr bond becomes significantly shorter, 2.705 Å for B3LYP and 2.682 for BP86, than for the other structures considered so far.

The thermodynamic instability is remedied by replacing the bridging carbonyl with two electrons; the result is $[(\mu\text{-H})_2Cr_2(CO)_8]^{2-}$ as shown in Figure 13. In this structure, the electrons are counted exactly the same as in $(\mu\text{-CO})(\mu\text{-H})_2Cr_2(CO)_8$, and the tribridging counting problem is remedied. As expected, the relative stability of this structure is 6.8 kcal/mol for B3LYP and 7.5 kcal/mol for BP86 with respect to dissociation to two $[Cr(CO)_4H]^-$ anions. Although the complex is more stable, the Cr−Cr bond and the terminal C−O bond distance are slightly longer than in the tribridged molecule. These results would indicate that the bridging carbonyl, not the electrons, destabilizes $(\mu\text{-CO})(\mu\text{-H})_2Cr_2(CO)_8$. This particular dianion is a more likely candidate for synthesis.

IV. Conclusions

Our results answer the question of why $Mn_2(CO)_{10}$ is relatively stable while $Cr_2(CO)_{11}$ is not. While it is somewhat surprising that the $Cr_2(CO)_{11}$ is slightly higher in energy than $Cr(CO)_6 + Cr(CO)_5$, one possibility is that the CO's in each Mn in $Mn_2(CO)_{10}$ are already too close, i.e., the four Mn−C−Os are almost touching the Mn−C−Os of the adjacent metal. [This should also be true of $Cr_2(CO)_{10}^{2-}$.] However, when a CO is added between the M−C−Os, as is done by introducing the 11th CO, the repulsion between the new CO and the M−Co's could be much higher, so the energy goes up. This could explain the high energy of the classic monobridged structure. The structure with two partially bridged carbonyls then would be a compromise between the two.

We may also be able to account for the stability of $[(\mu\text{-H})Cr_2(CO)_{10}]^-$. It may be thought of as $[(CO)_5Cr{-}Cr((CO)_5]^{2-}$ with a proton slipped between the two metal atoms with no consequence on the structure and with no additional strain. This could be similar to the Li−Li bond in Li_2 which may be protonated to the linear structure $Li{-}H{-}Li^+$ with almost the same Li−Li distance. Here the situation is the same. The Cr−Cr bond is being protonated, but since it is already a dianion, after protonation the molecule has one negative charge. No such new bond is generated when $Cr(CO)_6 + Cr(CO)_5$ interact to give $Cr_2(CO)_{11}$.

This may also account for the thermodynamic instability of $Cr_2(CO)_{11}$ structures and the observation of the more stable $[(\mu\text{-H})Cr_2(CO)_{10}]^-$. The potential energy surface is very flat for the $Cr_2(CO)_{11}$ structures. The BP86 method predicts this molecule to have a local minimum of C_s symmetry with two bridging carbonyls. This structure is thermodynamically unstable by 1.7 kcal/mol, lying above the chromium hexacarbonyl and pentacarbonyl fragments but slightly kinetically stable. The BP86 $Cr_2(CO)_{11}$ transition state for dissociation to $Cr(CO)_6 + Cr((CO)_5$ lies 1.9 kcal/mol above the local C_s minimum. The B3LYP method predicts dissociation without a barrier for the C_s symmetry structure likely due to the lesser amount of electron correlation from the HF component of this functional.

On the other hand, both functionals show that the $[(\mu\text{-H})Cr_2(CO)_{10}]^-$ structure is quite stable with respect to dissociation to fragments, but the two functionals produce somewhat different geometries. The B3LYP functional predicts a linear Cr−H−Cr bond while the BP86 functional predicts a bond of 147°, which is closer to the experimental angle of 159°. However, the experimental structures reflect the same ambiguity.

Tribridged structures for both $Cr_2(CO)_{11}$ and the $[Cr_2(CO)_{10}H]^-$ are predicted to lie much higher in energy than double or single bridging structures. However, the B3LYP and BP86 functionals give varying results for the energy differences of the molecule and fragments for the tribridging structures $(\mu\text{-CO})_3Cr_2(CO)_8$ and $[(\mu\text{-CO})_2(\mu\text{-H})Cr_2(CO)_8]^-$. The relative energies of the tribridged structures with respect to their fragments differ by about 20 kcal/mol for the two functionals. The number of imaginary harmonic vibrational frequencies also differs. The results do show unequivocally that tribridging structures of both $Cr_2(CO)_{11}$ and $[Cr_2(CO)_{10}H]^-$ are energetically high lying with respect to both the fragments and the mono- or dibridged structures and are therefore unlikely to be observed.

Of the structures examined, $[(\mu\text{-H})Cr_2(CO)_{10}]^-$ is found to be thermodynamically stable and the theoretical geometry determined by the BP86 functional to be in good agreement with experiment. Though not presently known, $[(\mu\text{-H})_2Cr_2(CO)_8]^{2-}$ may be observable owing to its thermodynamic stability. However, the unobserved $Cr_2(CO)_{11}$ will likely remain difficult to prepare since its energy lies above its fragments and its barrier to dissociation is low or zero. For similar reasons, the tribridged structures are also unlikely to be observed. Of course a loose complex of the type $Cr(CO)_6\cdots Cr(CO)_5$ should be observable at sufficiently low temperatures.

Acknowledgment. This work is supported in part by the U.S. National Science Foundation, Grant CHE-9815397. The authors sincerely thank Professor E. D. Jemmis for helpful insights into the reasons for stability differences. N.A.R. also is grateful to Joseph Kenny for help in the early phases of the project; to Jason Gonzales, Jingwei Qiao, and Nick Petraco for help in proofreading and editing; and to Dr. Yukio Yamaguchi for helpful discussions.

References and Notes

(1) Ford, T. A.; Huber, H.; Klotzbucher, W.; Moskovits, M.; Ozin, G. A. *Inorg. Chem.* **1976**, *15*, 1666.

(2) Ford, T. A.; Ozin, G. A. *Mol. Spectrosc. Dense Phases, Proc. Eur. Congr. Mol. Spectrosc.* **1975**, *12*, 389.

(3) Hanlan, L.; Huber, H.; Ozin, G. A. *Inorg. Chem.* **1976**, *15*, 2592.

(4) Burdett, J. K.; Graham, M. A.; Perutz, R. N.; Poliakoff, M.; Rest, A. J.; Turner, J. J.; Turner, R. F. *J. Am. Chem. Soc.* **1975**, *97*, 4805.

(5) Handy, L. B.; Treichel, P. M.; Dahl, L. F.; Hayter, R. G. *J. Am. Chem. Soc.* **1966**, *88*, 366.

(6) Roziere, J.; Williams, J. M.; Stewart, R. P., Jr.; Petersen, J. L.; Dahl, L. F. *J. Am. Chem. Soc.* **1977**, *99*, 4497.

(7) Handy, L. B.; Ruff, J. K.; Dahl, L. F. *J. Am. Chem. Soc.* **1970**, *92*, 7312.

(8) Petersen, J. L.; Brown, R. K.; Williams, J. M.; McMullan, R. K. *Inorg. Chem.* **1979**, *18*, 3493.

(9) Bombieri, G.; Bruno, G.; Grillone, M. D.; Polizzotti, X. *J. Organomet. Chem.* **1984**, *273*, 69.

(10) Hey-Hawkins, E.; von Schnering, H. G. *Chem. Ber.* **1991**, *124*, 1167.

(11) Lee, I.; Geib, S. J.; Cooper, N. H. *Acta Crystallogr., Sect. C* **1996**, *52*, 292.

(12) Borrmann, H.; Pirani, A. M.; Schrobilgen, G. J. *Acta Crystallogr., Sect. C* **1997**, *53*, 19.

(13) Petersen, J. L.; Masino, A.; Stewart, R. P., Jr. *J. Organomet. Chem.* **1981**, *208*, 55.

(14) Wilson, R. D.; Graham, S. A.; Bau, R. *J. Organomet. Chem.* **1975**, *91*, C49.

(15) Hart, D. W.; Bau, R.; Koetzle, T. F. *Organometallics* **1985**, *4*, 1590.

(16) King, R. B.; Lee, T. W. *Inorg. Chem.* **1982**, *21*, 319.

(17) King, R. B. *Acc. Chem. Res.* **1980**, *13*, 243.

(18) Newton, M. G.; King, R. B.; Lee, T. W.; Norskov-Lauritzen, L.; Kumar, V. *Chem. Commun.* **1982**, 201.

(19) King, R. B.; RaghuVeer, K. S. *Inorg. Chem.* **1984**, *23*, 2482.

(20) Ignatyev, I. S.; Schaefer, H. F.; King, R. B.; Brown, S. T. *J. Am. Chem. Soc.* **2000**, *122*, 1989.

(21) Xie, Y.; Schaefer, H. F.; King, R. B. *J. Am. Chem. Soc.* **2000**, *122*, 8746.

(22) Kenny, J. P.; Schaefer, H. F.; King, R. B. *Inorg. Chem.* **2001**, *40*, 900.

(23) Eyermann, C. J.; Chung-Phillips, A. *Inorg. Chem.* **1984**, *23*, 2025.

(24) Jezowska-Trzebiatowska, B.; Nissen-Sobocinska, B. *J. Organomet. Chem.* **1988**, *342*, 215.

(25) Jezowska-Trzebiatowska, B.; Nissen-Sobocinska, B. *J. Organomet. Chem.* **1989**, *376*, 69.

(26) Churchill, M. R.; Chang, S. W. *Inorg. Chem.* **1978**, *13*, 2413.

(27) Green, M. L. *J. Organomet. Chem.* **1995**, *500*, 127.

(28) Crabtree, R. H. *The Organometallic Chemistry of the Transition Metals*; John Wiley and Sons: New York, 2001.

(29) Dunning, T. H. *J. Chem. Phys.* **1970**, *53*, 2823.

(30) Huzinaga, S. *J. Chem. Phys.* **1965**, *42*, 1293.

(31) Wachters, A. J. H. *J. Chem. Phys.* **1970**, *52*, 1033.

(32) Hood, D. M.; Pitzer, R. M.; Schaefer, H. F. *J. Chem. Phys.* **1979**, *71*, 705.

(33) Jang, J. H.; Lee, J. G.; Lee, H.; Xie, Y. M.; Schaefer, H. F. *J. Phys. Chem. A* **1998**, *102*, 5298.

(34) Bauschlicher, C. W., Jr.; Ricca, A.; Partridge, H.; Langhoff, S. R. *Recent Advances in Density Functional Theory, Part II*; World Scientific Publishing: Singapore, 1997.

(35) Becke, A. D. *J. Chem. Phys.* **1993**, *98*, 5648.

(36) Lee, C.; Yang, W.; Parr, R. G. *Phys. Rev. B* **1988**, *37*, 785.

(37) Becke, A. D. *Phys. Rev. A* **1988**, *38*, 3098.

(38) Perdew, J. P. *Phys. Rev B* **1986**, *33*, 8822.

(39) Frisch, M. J.; Trucks, G. W.; Schlegel, H. B.; Gill, P. M. W.; Johnson, B. G.; Robb, M. A.; Cheeseman, J. R.; Keith, T.; Petersson, G. A.; Montgomery, J. A.; Raghavachari, K.; Al-Laham, M. A.; Zakrzewski, V. G.; Ortiz, J. V.; Foresman, J. B.; Cioslowski, J.; Stefanov, B. B.; Nanayakkara, A.; Challacombe, M.; Peng, C. Y.; Ayala, P. Y.; Chen, W.; Wong, M. W.; Andres, J. L.; Replogle, E. S.; Gomperts, R.; Martin, R. L.; Fox, D. J.; Binkley, J. S.; Defrees, D. J.; Baker, J.; Stewart, J. P.; Head-Gordon, M.; Gonzalez, C.; Pople, J. A. *Gaussian 94*, revision c.3; Gaussian, Inc.: Pittsburgh, PA, 1995.

(40) Persson, B. J.; Roos, B. O.; Pierloot, K. *J. Phys. Chem.* **1994**, *101*, 6810.

(41) Menconi, G.; Wilson, P. J.; Tozer, D. J. *J. Chem. Phys.* **2001**, *114*, 3958.

(42) Jost, A.; Rees, B.; Yelon, W. B. *Acta Crystallogr., Sect. B* **1975**, *31*, 2649.

(43) Rees, B.; Mitschler, A. *J. Am. Chem. Soc.* **1976**, *98*, 7918.

(44) Spears, K. G. *J. Phys. Chem.* **1997**, *101*, 6273.

(45) Jonas, V.; Thiel, W. *J. Chem. Phys.* **1995**, *102*, 8474.

(46) Ehlers, A. W.; Frenking, G. *J. Am. Chem. Soc.* **1994**, *116*, 1514.

(47) Barnes, L. A.; Rosi, M.; Bauschlicher, C. W., Jr. *J. Chem. Phys.* **1991**, *94*, 2031.

(48) Barnes, L. A.; Liu, B.; Lindh, R. *J. Chem. Phys.* **1993**, *98*, 3978.

(49) Darensbourg, M. Y.; Bau, R.; Marks, M. W.; Burch, R. R., Jr.; Deaton, J. C.; Slater, S. *J. Am. Chem. Soc.* **1982**, *104*, 6961.

(50) Liddell, M. J. *J. Organomet. Chem.* **1995**, *102*, 8474.

(51) Hedberg, K.; Schomaker, V. *J. Am. Chem. Soc.* **1951**, *73*, 1482.

(52) Broach, R.; Williams, J. M. *Inorg. Chem.* **1979**, *18*, 314.

(53) Orpen, A. G.; Rivera, A. V.; Bryan, E. G.; Pippard, D.; Sheldrick, G. M. *J. Chem. Soc., Chem. Commun.* **1988**, 723.

(54) Kubas, G. J. *Acc. Chem. Res.* **1988**, *18*, 120.